

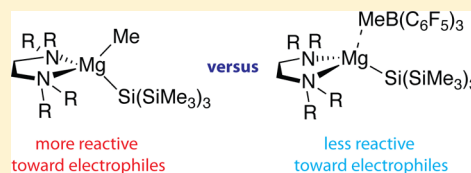
Nucleophilicity of Neutral versus Cationic Magnesium Silyl Compounds

KaKing Yan, Brianna M. Upton, Jing Zhu, Arkady Ellern, and Aaron D. Sadow*

Department of Chemistry, Iowa State University, 1605 Gilman Hall, Ames Iowa 50011, United States

S Supporting Information

ABSTRACT: Charge and ancillary ligands affect the reactivity of monomeric tris(trimethylsilyl)silyl magnesium compounds. Diamine-coordinated (tmeda)-Mg{Si(SiMe₃)₃}Me (tmeda = tetramethylethylenediamine; **2-tmeda**) and (dpe)Mg{Si(SiMe₃)₃}Me (dpe = 1,2-*N,N*-dipyrrolideneethane; **2-dpe**) are synthesized by salt elimination reactions of L₂MgMeBr and KSi(SiMe₃)₃. Compounds **2-tmeda** or **2-dpe** react with MeI or MeOTf to give MeSi(SiMe₃)₃ as the product of Si–C bond formation. In contrast, **2-tmeda** and **2-dpe** undergo exclusively reaction at the magnesium methyl group with electrophiles such as Me₃SiI, B(C₆F₅)₃, HB(C₆F₅)₂, and [Ph₃C][B(C₆F₅)₄]. These reactions provide a series of neutral, zwitterionic, and cationic magnesium silyl compounds, and from this series we have found that silyl group transfer is less effective with cationic magnesium compounds than neutral complexes.



INTRODUCTION

The highly polar metal–carbon bonds in alkali and alkaline earth metal organometallic compounds are central to their strongly nucleophilic and highly basic character.¹ Metal silyl compounds of groups 1 and 2 might be expected to have similar nucleophilic and basic character based on their use in salt metathesis chemistry.² Some distinctions between M–C and M–Si compounds are evident in d⁰ early transition metal chemistry, however, as the early metal–silicon bond is expected to be less polar,³ longer, and weaker^{4,5} than corresponding early metal–carbon bonds; the latter two points suggest that early metal silyls will react more rapidly than metal alkyls, as is observed for σ -bond metathesis reactions involving organosilanes or reactions with H₂.⁶ In contrast, increased polarity might imply that early metal alkyls should have greater nucleophilicity than silyls, and in fact alkene insertions into metal–carbon bonds are well established in olefin polymerizations but related reactions of d⁰ metal–silicon bonds are not.⁷ Direct comparisons between reactions of silyl and alkyl species are complicated by the difficulty in preparing organometallic compounds that are identical in all respects (metal center, ancillary ligands, and groups bonded to the carbon or silicon atom) aside from the M–E moiety itself.⁸ In preparation for such studies, we decided to compare the reactivity of monomeric mixed silyl alkyl magnesium compounds with a series of electrophiles. We chose magnesium as the metal center because bonding would not be complicated by M–E π bonding or metal–ligand secondary interactions, as well as our interest in developing catalytic chemistry of main group metals.

The compound (THF)₂MgSi(SiMe₃)₃Me⁹ shows that mixed silyl alkyl magnesium complexes are isolable. Although the steric properties of the Si(SiMe₃)₃ versus the methyl group might be expected to dominate reactivity patterns, an initial data point from Marschner and co-workers suggests otherwise.⁹ The salt metathesis reaction of (THF)₂Mg{Si(SiMe₃)₃}Me and

Cp₂ZrCl₂ generates the intermediate Cp₂Zr{Si(SiMe₃)₃}Cl rather than Cp₂ZrMeCl on the pathway to the Cp₂ZrSi(SiMe₃)₃Me final product.¹⁰ Thus, the bulkier silyl group transfers faster than the methyl group, although both groups undergo transmetalation. Changes in reaction conditions, ancillary ligands, and identity of the electrophile might change the relative rates of group transfer and thus control selectivity in bond forming reactions.

In this study, we prepared diamine-coordinated compounds (tmeda)Mg{Si(SiMe₃)₃}Me (tmeda = tetramethylethylenediamine; **2-tmeda**) and (dpe)MgSi(SiMe₃)₃Me (dpe = dipyrrolidene ethane; **2-dpe**) to stabilize monomeric structures and potentially support low-coordinate magnesium centers. The interactions of these two magnesium compounds and a series of electrophiles have been investigated to compare the reactivity of Mg–Si and Mg–Me bonds. We were curious about the products of reactions of **2-tmeda** or **2-dpe** and Lewis acid electrophiles such as B(C₆F₅)₃ or [Ph₃C][B(C₆F₅)₄] that might provide either silyl or alkyl magnesium cationic compounds. Despite the highly electropositive nature of divalent magnesium, few cationic organomagnesium compounds have been described,¹¹ and we are not aware of cationic compounds containing a Mg–Si bond. These species are interesting because cationic alkyl and silyl early transition metal compounds show enhanced reaction rates in comparison to neutral analogues in σ -bond metathesis-type reactions involving Si–H and C–H bonds,¹² and cationic group 4 alkyl compounds are well-known to readily insert olefins.¹³ This trend, however, is less established for neutral versus cationic magnesium alkyl compounds. Recently, cationic magnesium butyl complexes were

Special Issue: Applications of Electrophilic Main Group Organometallic Molecules

Received: May 20, 2013

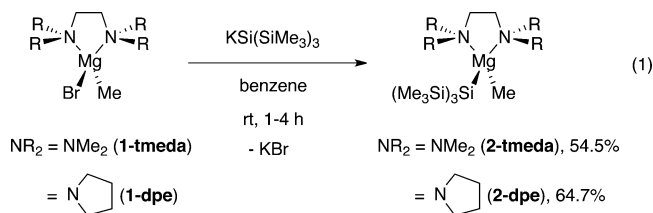
Published: July 15, 2013

shown to be effective initiators for caprolactone ring-opening polymerization,^{11c,d} but the relative reactivity of neutral, zwitterionic, and cationic catalysts is not clearly addressed.

The present study demonstrates that ancillary ligands, charge, and the electrophilic partner affect the relative reactivity of Mg–Me versus Mg–Si(SiMe₃)₃ groups. Furthermore, we have found that reactions of (L₂)Mg{Si(SiMe₃)₃}Me with B(C₆F₅)₃ and [Ph₃C][B(C₆F₅)₄] provide the first examples of cationic compounds that contain a magnesium–silicon bond, and this allows a direct comparison of reactivity of neutral silyl alkyl magnesium versus cationic silyl magnesium complexes.

RESULTS AND DISCUSSION

1. Synthesis and Characterization of (tmeda)Mg{Si(SiMe₃)₃}Me and (dpe)Mg{Si(SiMe₃)₃}Me. The complex (tmeda)MgMeBr (**1-tmeda**) is a convenient starting material, as it is an isolable, well-defined solid.¹⁴ The reaction of **1-tmeda** and KSi(SiMe₃)₃ in benzene yields (tmeda)Mg{Si(SiMe₃)₃}Me (**2-tmeda**) (eq 1). This route follows a sequence previously established for (THF)₂Mg{Si(SiMe₃)₃}Me.¹⁰ We also prepared (dpe)MgMeBr (dpe = 1,2-*N,N*-dipyrrolideneethane) (**1-dpe**) by addition of dpe to a solution of MgMeBr as a magnesium starting material with a potentially bulkier and more electron-donating diamine ligand (see below for a steric comparison). The reaction of **1-dpe** and KSi(SiMe₃)₃ affords (dpe)Mg{Si(SiMe₃)₃}Me (**2-dpe**) (eq 1).



The ¹H, ¹³C{¹H} and ²⁹Si NMR spectra of **2-tmeda** and **2-dpe** have similar chemical shifts for the silyl groups. In addition, the ²⁹Si NMR chemical shifts of the central silicon (i.e., Si(SiMe₃)₃) of –175.4 and –177.0 ppm in the tmeda and dpe magnesium silyl compounds (see Table 1) are similar to the value reported for (THF)₂Mg{Si(SiMe₃)₃}Me (–174.5 ppm).¹⁰

The magnesium methyl resonances appear upfield of tetramethylsilane in both the tmeda and dpe compounds at –1.03 and –1.02 ppm, respectively. These signals are further upfield than the magnesium methyl in (THF)₂Mg{Si(SiMe₃)₃}Me that appears at –0.8 ppm.¹⁰

A single crystal X-ray diffraction study of **2-tmeda** highlights its monomeric nature and the four coordinate magnesium center (see Figure 1). The solid-state structure of (THF)₂Mg-

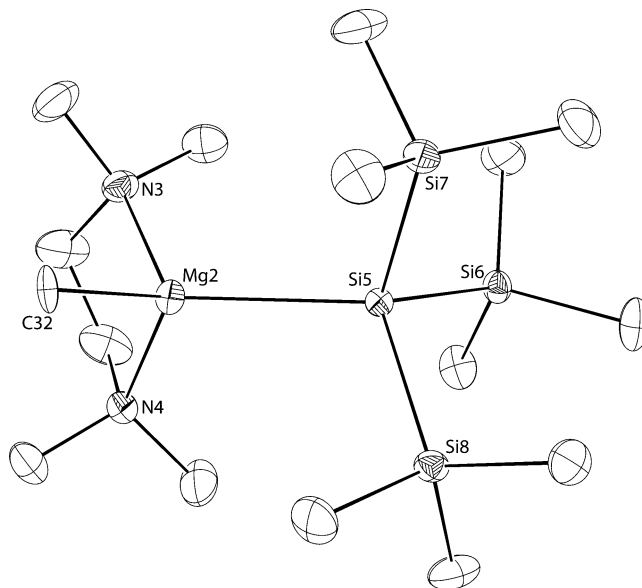


Figure 1. ORTEP diagram of **2-tmeda**. Ellipsoids are plotted at 35% probability. The unit cell contains two crystallographically independent molecules, and only one is illustrated. The Mg–X distances are identical within error for the two molecules, and the X–Mg–X bond angles are within 1°. Hydrogen atoms were not included in the plot for clarity. Selected interatomic distances (Å): Mg2–Si5, 2.6414(9); Mg2–C32, 2.222(2); Mg–N3, 2.210(2); Mg–N4, 2.213(2). Selected interatomic angles (deg): Si5–Mg2–C32, 120.73(6); N3–Mg2–N4, 82.67(8); N3–Mg2–Si5, 115.34(6); N4–Mg2–Si5, 112.69(5).

{Si(SiMe₃)₃}Me is not reported, but those of (tmeda)Mg{Si(SiMe₃)₃}₂, (THF)₂Mg{Si(SiMe₃)₃}Ph, and (THF)₂Mg{Si(SiMe₃)₃}₂ are previously described.¹⁰ The chelating tmeda ligand gives a N–Mg–N angle of 82.67(8)° in **2-tmeda**, which is similar to the value for (tmeda)Mg{Si(SiMe₃)₃}₂ of 81.8(3)°,¹⁰ whereas the unconstrained O–Mg–O angles in (THF)₂Mg{Si(SiMe₃)₃}Ph¹⁰ and (THF)₂Mg{Si(SiMe₃)₃}₂⁹ are wider at 95.4(1)° and 92.0(3)°, respectively. This change between chelated and independent ancillary ligand L–Mg–L angle apparently affects the Si–Mg–C angle. Thus, the Si–Mg–C_{ph} angle of 128.2(1) in the latter compound is greater than the 120.73(6) angle in **2-tmeda**. Space-filling models show that there is space between phenyl and tris(trimethyl)silyl groups in

Table 1. ¹H NMR and ²⁹Si NMR Chemical Shifts of Magnesium Silyl Compounds

compound	δ Si(SiMe ₃) ₃	δ Si(SiMe ₃) ₃
(tmeda)Mg{Si(SiMe ₃) ₃ }Me (2-tmeda)	0.51	–175.4
(dpe)Mg{Si(SiMe ₃) ₃ }Me (2-dpe)	0.51	–177.0
(tmeda)Mg{Si(SiMe ₃) ₃ }I (3-tmeda)	0.50	–167.9
(dpe)Mg{Si(SiMe ₃) ₃ }I (3-dpe)	0.51	–168.9
(tmeda)Mg{Si(SiMe ₃) ₃ }MeB(C ₆ F ₅) ₃ (4-tmeda)	0.18	–167.2
(dpe)Mg{Si(SiMe ₃) ₃ }MeB(C ₆ F ₅) ₃ (4-dpe)	0.24	–168.7
(tmeda)Mg{Si(SiMe ₃) ₃ }IB(C ₆ F ₅) ₃ (5-tmeda)	0.36	–165.0
[(tmeda)MgSi(SiMe ₃) ₃][B(C ₆ F ₅) ₄] (6-tmeda)	0.28	–163.4
[(dpe)MgSi(SiMe ₃) ₃][B(C ₆ F ₅) ₄] (6-dpe)	0.30	–170.8
(tmeda)Mg{Si(SiMe ₃) ₃ }(μ-H) ₂ B(C ₆ F ₅) ₂ (7-tmeda)	0.28	–173.1
(dpe)Mg{Si(SiMe ₃) ₃ }(μ-H) ₂ B(C ₆ F ₅) ₂ (7-dpe)	0.30	–173.1

(THF)₂Mg{Si(SiMe₃)₃}Ph and between methyl, tris(trimethyl)silyl, and tmeda ligands in **2-tmeda**. Furthermore, solid angle calculations (see below) using the program Solid-G show that tmeda, Me, and Si(SiMe₃)₃ ligands together occupy only ca. 80% of the space surrounding the magnesium center in **2-tmeda**, and there are no unfavorable interligand interactions.¹⁵ Likewise, only 78% of the space around the magnesium center in (THF)₂Mg{Si(SiMe₃)₃}Ph is occupied. Thus, intramolecular steric effects are apparently not responsible for the change in Si–Mg–C angles between (THF)₂Mg{Si(SiMe₃)₃}Ph and **2-tmeda**; the changes are attributed to the effect of the chelating tmeda on the two other ligands, even in a complex with highly polarized bonding.

The Mg–Si distance in **2-tmeda** is 2.6414(9) Å, and the Mg–Si distances for the crystallographically characterized compounds of this report are listed in Table 2. For comparison, the Mg–Si distance in THF₂MgSi(SiMe₃)₃Ph is 2.650(2) Å.¹⁰

Table 2. Mg–Si Interatomic Distances of Neutral and Cationic Magnesium Silyl Compounds

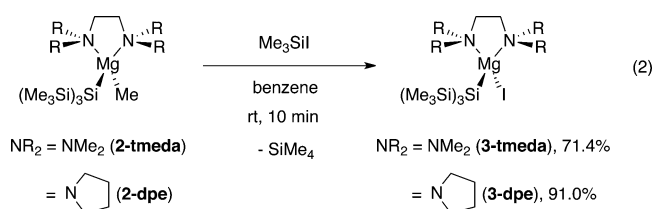
compound	Mg–Si distance (Å)
(tmeda)Mg{Si(SiMe ₃) ₃ }Me (2-tmeda)	2.6414(9)
(dpe)Mg{Si(SiMe ₃) ₃ }I (3-dpe)	2.609(2)
(tmeda)Mg{Si(SiMe ₃) ₃ }MeB(C ₆ F ₅) ₃ (4-tmeda)	2.576(2)
(dpe)Mg{Si(SiMe ₃) ₃ }MeB(C ₆ F ₅) ₃ (4-dpe)	2.602(2)
(tmeda)Mg{Si(SiMe ₃) ₃ }(μ -H ₂)B(C ₆ F ₅) ₂ (7-tmeda)	2.648(1)

2. Reactions of (tmeda)Mg{Si(SiMe₃)₃}Me or (dpe)Mg{Si(SiMe₃)₃}Me and Electrophiles. Scheme 1 summarizes the transformations of (L₂)Mg{Si(SiMe₃)₃}Me (L₂ = tmeda or dpe) and electrophiles in the context of methyl versus silyl group transfer. Reactions of **2-tmeda** or **2-dpe** and MeOTf in benzene afford (Me₃Si)₃SiMe and (L₂)Mg(OTf)Me within 5 min at room temperature. The ¹H NMR chemical shifts of the MgMe in (tmeda)Mg(OTf)Me and (dpe)Mg(OTf)Me are 0.20 and 0.12 ppm in benzene-*d*₆, respectively. Addition of excess MeOTf (>2 equiv) slowly gives ethane (0.8 ppm in benzene-*d*₆) and a white precipitate, presumed to be

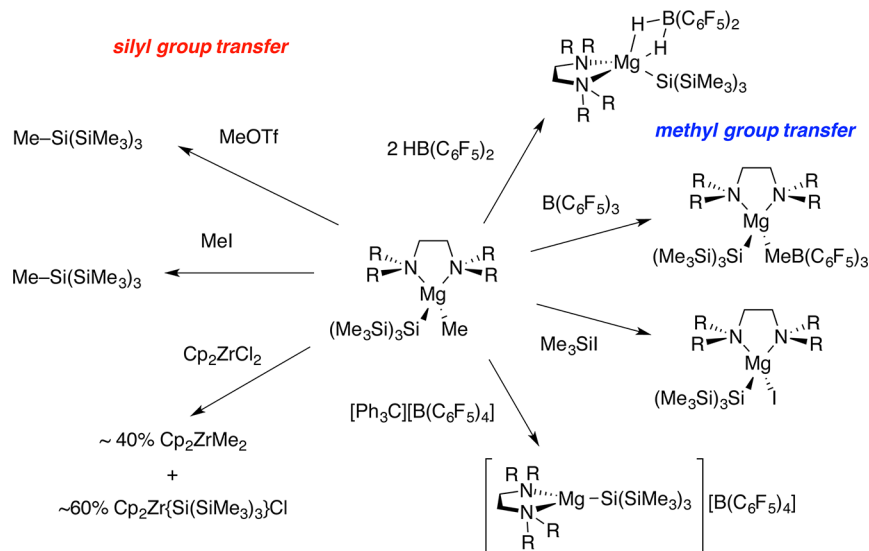
(L₂)Mg(OTf)₂, after 30 min, in addition to the (Me₃Si)₃SiMe formed instantaneously. Compounds **2-tmeda** or **2-dpe** and MeI also react at room temperature, but the reactions take longer (18 h at room temperature) to give full conversion to (Me₃Si)₃SiMe.

The rates of formation of Me–Si(SiMe₃)₃ versus Me–Me follow the expectations previously established by the reaction of Cp₂ZrCl₂ and (THF)₂Mg{Si(SiMe₃)₃}Me, for which salt metathesis with the bulky tris(trimethylsilyl)silyl group is kinetically favored over methyl group transfer.¹⁰ In contrast, reaction of **2-tmeda** and Cp₂ZrCl₂ initially affords a mixture of Cp₂Zr{Si(SiMe₃)₃}Cl, Cp₂ZrMe₂, and Cp₂Zr{Si(SiMe₃)₃}Me in a 10:7:1 ratio and a ~1:1 mixture of (tmeda)Mg{Si(SiMe₃)₃}Cl and (tmeda)MgCl₂. Magnesium methyl resonances, which are typically far upfield (~ -1 ppm) even compared to Cp₂ZrMe₂ (-0.13 ppm, benzene-*d*₆),¹⁶ are not detected in the reaction mixture. The species (tmeda)MgCl₂ is soluble in the reaction mixture and assigned on the basis of the distinct chemical shifts of tmeda resonances in the ¹H NMR spectrum from those of a benzene-*d*₆ solution of authentic tmeda and the starting materials. Interestingly, the reaction mixture is converted to Cp₂Zr{Si(SiMe₃)₃}Me as the sole zirconium product after 12 h at room temperature. In addition, the reaction of **2-dpe** and Cp₂ZrCl₂ initially gives a mixture of Cp₂Zr{Si(SiMe₃)₃}Cl, Cp₂ZrMe₂, and Cp₂Zr{Si(SiMe₃)₃}Me in a 3.4:5.2:1 ratio en route to Cp₂Zr{Si(SiMe₃)₃}Me. Thus, the ancillary diamine ligands increase the nucleophilicity of the methyl group versus the silyl group in comparison to the THF-coordinated compound in transmetalation reactions.¹⁰

This trend is further evidenced by reactions of **2-tmeda** or **2-dpe** and Me₃SiI that afford the silyl–Grignard complexes (tmeda)Mg{Si(SiMe₃)₃}I (**3-tmeda**) or (dpe)Mg{Si(SiMe₃)₃}I (**3-dpe**) and SiMe₄ (eq 2). The methyl magnesium iodide and



Scheme 1. Reactions of (L₂)Mg{Si(SiMe₃)₃}Me and Electrophiles Showing Reagents That Interact with the Silyl Group and Those That Interact with the Methyl Group



$\text{Si}(\text{SiMe}_3)_4$, as another possible set of products, were not detected in the ^1H NMR spectra of the crude reaction mixtures. A ^1H NMR spectrum acquired 10 min after mixing **2-tmeda** and Me_3SiI (1.1 equiv) in benzene- d_6 revealed rapid and quantitative formation of Me_4Si and new resonances assigned to **3-tmeda**.

On preparative scale, **3-tmeda** and **3-dpe** are readily isolated by evaporation of the volatile materials followed by extraction and crystallization from toluene. The X-ray crystal structure of **3-dpe** highlights its monomeric nature, and there are no close contacts between $(\text{dpe})\text{Mg}\{\text{Si}(\text{SiMe}_3)_3\}\text{I}$ molecules (see Figure 2).

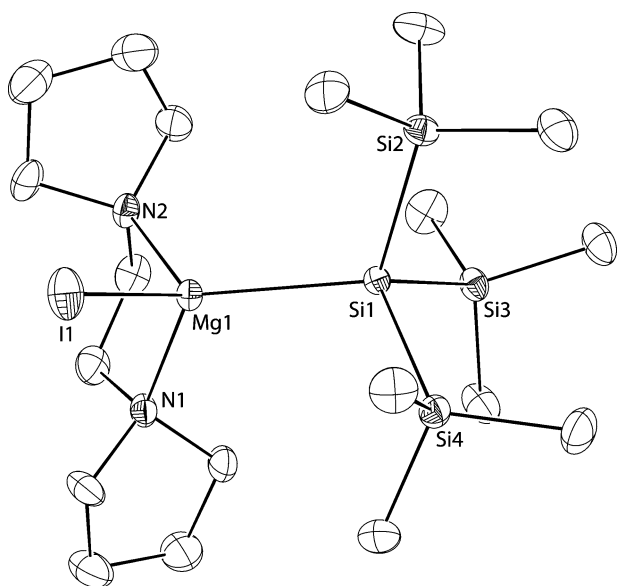


Figure 2. ORTEP diagram of **3-dpe** plotted at 35% probability. A co-crystallized benzene molecule and hydrogen atoms were not included. Selected interatomic distances (Å): Mg1–Si1, 2.609(2); Mg1–I1, 2.723(2); Mg1–N1, 2.173(4); Mg1–N2, 2.180(4). Selected interatomic angles (deg): Si1–Mg1–I1, 114.08(6); N1–Mg1–N2, 83.5(2).

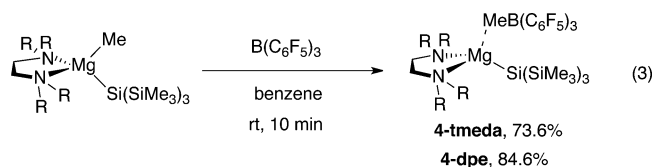
The Mg1–Si1 distance of 2.609(2) Å is 0.03 Å shorter than the Mg2–Si5 distance (2.6414(9) Å) in **2-tmeda**.

The ^1H NMR spectra of **3-tmeda** or **3-dpe** dissolved in benzene- d_6 are unchanged after heating (in sealed NMR tubes) at 115 °C for 5 h. Compounds **3-tmeda** and **3-dpe** are robust in the absence of protic reagents and air, and resistant toward disproportionation, and do not show evidence of dissociation of the diamine ligand. Reactions of 3 equiv of Me_3SiI and **2-tmeda** or **2-dpe** at room temperature provide **3-tmeda** or **3-dpe** as the only observed $(\text{Me}_3\text{Si})_3\text{Si}$ - or diamine-containing species. Upon heating these reaction mixtures at 83 °C in benzene- d_6 , $\text{Si}(\text{SiMe}_3)_4$ is slowly formed, giving 83% conversion after 28 h. Strangely, MeOTf (2 equiv) and **3-tmeda** or **3-dpe** react at room temperature to give $\text{HSi}(\text{SiMe}_3)_3$ as the major product along with $\text{MeSi}(\text{SiMe}_3)_3$ and a white precipitate. Although we currently have no explanation for this result, we repeated the experiments several times with carefully surface silylated and oven-dried glassware (these techniques were suitable for handling **3-tmeda** in the absence of MeOTf), as well as dried MeOTf that gives nonhydrolytic reactivity with **2-tmeda** or **2-dpe**. Perhaps even more surprisingly, only starting materials are observed after treatment of either **2-tmeda** or **2-dpe** with Me_3SiOTf .

Thus, the magnesium silyl moiety in diamine-coordinated compounds is more reactive to smaller electrophiles (MeOTf)

than the methyl group, significantly less reactive toward larger electrophiles (Cp_2ZrCl_2 and Me_3SiI) than the methyl group, and unexpectedly inert toward some electrophiles (Me_3SiOTf). Following this idea, we began to explore reactions with other main group electrophiles to form zwitterionic or cationic magnesium silyl species.

3. Reactions of $\text{B}(\text{C}_6\text{F}_5)_3$ and $(\text{tmeda})\text{Mg}\{\text{Si}(\text{SiMe}_3)_3\}\text{Me}$ or $(\text{dpe})\text{Mg}\{\text{Si}(\text{SiMe}_3)_3\}\text{Me}$. Reaction of **2-tmeda** and $\text{B}(\text{C}_6\text{F}_5)_3$ in benzene provides benzene- and toluene-soluble $(\text{tmeda})\text{Mg}\{\text{Si}(\text{SiMe}_3)_3\}\text{MeB}(\text{C}_6\text{F}_5)_3$ (**4-tmeda**; eq 3), which is readily isolated by solvent evaporation. The ^1H NMR resonance from $\text{MeB}(\text{C}_6\text{F}_5)_3$ appeared at 1.67 ppm, which was shifted by 2.7 ppm downfield in comparison to the neutral magnesium methyl precursor (−1.03 ppm). The B–Me interaction was unambiguously established by a ^1H – ^{11}B HMBIC experiment that contained a crosspeak between the broad ^1H NMR methyl resonance and the ^{11}B NMR resonance at −14.3 ppm. The chemical shifts of the $-\text{Si}(\text{SiMe}_3)_3$ group in the ^1H and ^{29}Si NMR spectra, however, were similar for **2-tmeda**, **3-tmeda**, and **4-tmeda**. Thus, the data indicate that $\text{B}(\text{C}_6\text{F}_5)_3$ interacts exclusively with the methyl group. Similarly, reaction of **2-dpe** and $\text{B}(\text{C}_6\text{F}_5)_3$ provides $(\text{dpe})\text{Mg}\{\text{Si}(\text{SiMe}_3)_3\}\text{MeB}(\text{C}_6\text{F}_5)_3$ (**4-dpe**) in 84.6% yield; however, **4-dpe** is formed as an insoluble oil that precipitates from benzene.



The solution structure of **4-tmeda** was probed to identify the magnesium center's coordination environment. Its room temperature ^1H and $^{13}\text{C}\{^1\text{H}\}$ NMR spectra (benzene- d_6) contained one singlet assigned to four equivalent methyl groups and one singlet assigned to the methylene moiety of the tmeda ligand suggesting effective pseudo- C_{2v} symmetry. In contrast, the NMe_2 groups are inequivalent in the four-coordinate compounds **2-tmeda** and **3-tmeda**. The two ^1H NMR resonances for **4-tmeda** are broad at 190 K indicating that tmeda is involved in a rapid, fluxional process even at that temperature. The fluxional process could involve formation or dissociation of a $\text{Mg}\cdots\text{MeB}(\text{C}_6\text{F}_5)_3$ interaction or conformational interconversions of the five-membered chelate ring. From 180 to 295 K, the $\text{MeB}(\text{C}_6\text{F}_5)_3$ resonance does not shift and only broadens slightly as the temperature is lowered. These data suggest that the $\text{Mg}\cdots\text{MeB}(\text{C}_6\text{F}_5)_3$ interaction in **4-tmeda** is labile in aromatic hydrocarbon solvents. For comparison, Marks's studies of ion-pair separation and methide transfer in $(\text{C}_5\text{H}_3\text{Me}_2)_2\text{ZrMe}(\mu\text{-Me})\text{B}(\text{C}_6\text{F}_5)_3$ indicate that ion-pair separation is 10 \times faster than borane dissociation in toluene- d_8 ;¹⁷ furthermore, the decoupling of diastereotopic ^1H NMR signals in $(\text{C}_5\text{H}_3\text{Me}_2)_2\text{Zr}\{\text{CH}(\text{SiMe}_3)_2\}[\text{MeB}(\text{C}_6\text{F}_5)_3]$ is beyond the limits of the low temperature point of toluene- d_8 suggestive of significant ionic character.^{17b} Studies of diketiminate-coordinated $[\text{Sc}]\text{Me}(\mu\text{-Me})\text{B}(\text{C}_6\text{F}_5)_3$ ion-pairs show that borane dissociation is not facile with more electropositive metal complexes; however, processes involving $\text{MeB}(\text{C}_6\text{F}_5)_3$ dissociation from the scandium center are sufficiently slow that they can be studied by ^1H NMR spectroscopy.¹⁸

The ^{19}F NMR chemical shift difference for *meta* and *para* fluorine resonances in **4-tmeda** is 4.0 ppm in benzene- d_6

and 3.9 ppm in bromobenzene- d_5 . Previously, Horton suggested that a $\Delta(\delta_{paraF} - \delta_{metaF})$ value greater than 3.5 ppm corresponds to an inner sphere interaction (Zr–Me–B, the so-called contact ion-pair), whereas $\Delta(\delta_{paraF} - \delta_{metaF}) < 3.5$ ppm indicates that a solvent-separated ion-pair is formed.¹⁹ By this measure, **4-tmeda** is best described as (tmeda)Mg{Si(SiMe₃)₃}(μ -Me)B(C₆F₅)₃, whereas the $\Delta(\delta_{paraF} - \delta_{metaF})$ in **4-dpe** is 2.8 ppm in bromobenzene- d_5 suggesting the structure [(dpe)MgSi(SiMe₃)₃][MeB(C₆F₅)₃]. While the relative solubility of the two compounds in aromatic hydrocarbon solvents follows the trend suggested by the $\Delta(\delta_{paraF} - \delta_{metaF})$ parameter, and **4-dpe** is significantly more soluble in bromobenzene- d_5 than in benzene- d_6 , one might expect that the structure, and thus the ¹⁹F NMR-based parameter, would be affected by solvent polarity. That is not the case, and this parameter for **4-tmeda** is apparently unaffected by a solvent change from benzene- d_6 to bromobenzene- d_5 . In that context, it is also worth noting that the ¹¹B NMR chemical shifts for **4-tmeda** (–15.1 ppm, bromobenzene- d_5) and **4-dpe** (–14.8 ppm, bromobenzene- d_5) are very similar but not identical. Additionally, the diffusion constant values *D* for **4-tmeda**, measured using PFG-spin echo experiments in benzene- d_6 at room temperature,²⁰ determined for the Si(SiMe₃)₃ group are within error of the values determined for [MeB(C₆F₅)₃]. Also, the diffusion constant values for the Si(SiMe₃)₃ and MeB(C₆F₅)₃ groups are identical in **4-dpe**, but distinct from **4-tmeda**. The observation that the cationic and anionic portions of these species diffuse at the same rate suggests that they are associated in solution, as expected for oppositely charged ions.

In the solid state, both **4-tmeda** and **4-dpe** contain zwitterionic, bridging Mg–Me–B(C₆F₅)₃ structures (see ORTEP diagrams in Figures 3 and 4). The Mg–N bonds are shorter by ca. 0.05 Å in the zwitterionic compounds than in the neutral precursor compounds. Interestingly, the Mg–Si distance is 0.065 Å shorter in zwitterionic **4-tmeda** than in neutral **2-tmeda** (Table 2). However, in **3-dpe** and **4-dpe**, the Mg–Si bond lengths are identical within error. In contrast, the Hf–Si distance is longer in Cp₂Hf(Si^tBuPh₂)(μ -Me)B(C₆F₅)₃ (2.851(3) Å) than in Cp₂Hf(Si^tBuPh₂)Me (2.835(2) Å).^{12d} The ionic radius of four coordinate magnesium(II) (0.57 Å) is only slightly less than that of hafnium(IV) (0.58 Å) and zirconium(IV) (0.59 Å).²¹

The Mg–C distance in **4-tmeda** (2.448(4) Å) is ca. 0.23 Å longer than in **2-tmeda**, and the distance in **4-dpe** is even longer at 2.459(4) Å. The objectively located and refined hydrogen atoms on the methyl groups are directed toward the magnesium center in both **4-tmeda** and **4-dpe**. Another interesting structural change between **2-tmeda** and **4-tmeda** is the N–Mg–Si angles, which are larger in methide-abstracted **4-tmeda** (119.7(1)° and 123.2(1)°) than in **2-tmeda** (112.69(6)° and 115.34(6)°) by ca. 7°. Space-filling models suggest that interligand interactions are minor for both **2-tmeda** and **4-tmeda**.

The compounds **4-tmeda** and **4-dpe** have similar constitution, except for the different diamine ancillary ligand, and both are crystallographically characterized. Therefore, we evaluated the relative steric properties of the two ligands using the X-ray coordinates and the program Solid-G to calculate the solid angles.¹⁵ The calculated solid angle for a ligand, given in steradians and reporting the surface area of a shadow cast by the ligand on the inside of a sphere surrounding the complex,²² is slightly larger for dpe (5.36 steradians) than tmeda (4.65 steradians), where the total surface area of a sphere is 12.56 steradians. Thus, the steric effect of dpe is ca. 6% larger

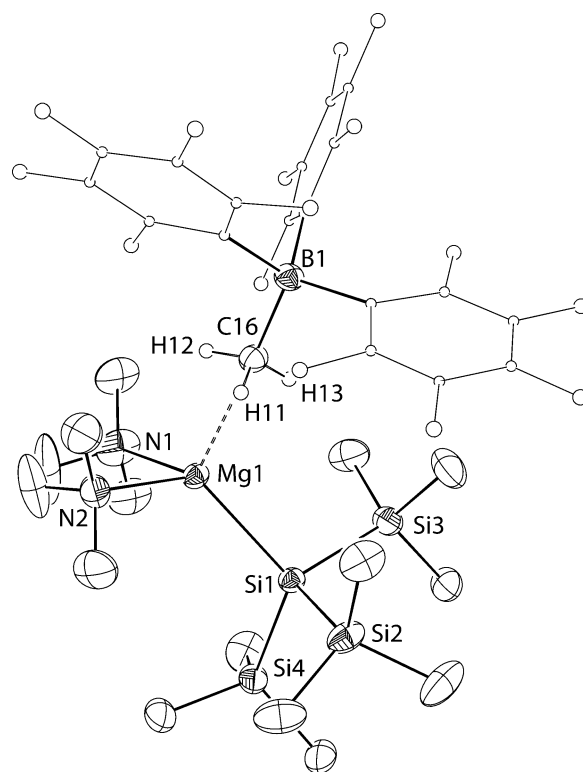


Figure 3. ORTEP diagram of (tmeda)Mg{Si(SiMe₃)₃}MeB(C₆F₅)₃ (**4-tmeda**) drawn at 35% probability. Hydrogen atoms on the MeB(C₆F₅)₃ were located objectively in the Fourier difference map, refined isotropically, and included in the plot. All other H are not plotted, nor are co-crystallized toluene molecules. Fluorine atoms and carbon atoms on MeB(C₆F₅)₃ are refined anisotropically and have normal thermal parameters but are depicted using a ball-and-stick representation for clarity. Selected distances (Å): Mg1–Si1, 2.576(2); Mg1–N1, 2.152(4); Mg1–N2, 2.165(4); Mg1–C16, 2.448(5); Mg1–H11, 2.30(4); Mg1–H12, 2.25(4); Mg1–H13, 2.40(4); B1–C16, 1.661(6). Selected angles (deg): N1–Mg1–N2, 84.7(2); Si1–Mg1–C16, 113.0; Mg1–C16–B1, 175.7(3).

than tmeda as described by the solid angle method, at least in these magnesium compounds.

The solid-state structures of zwitterionic **4-tmeda** and **4-dpe** clearly are not equivalent to the fluxional solution-phase structures. In particular, the $\Delta(\delta_{paraF} - \delta_{metaF})$ ¹⁹F NMR analysis and its solubility in toluene suggested that **4-dpe** is a solvent-separated ion-pair, while X-ray diffraction indicates that **4-dpe** packs in crystalline form as a contact ion-pair. The bridging Mg–Me–B structure and solvent-separated ion-pair structure are both probably important components of the magnesium compounds' solution structures.

The reaction of **4-tmeda** with the electrophile Me₃SiI provides another comparison with neutral **2-tmeda**. As with the neutral reactant, SiMe₄ is formed; however, the reaction time was much longer for **4-tmeda** than for **2-tmeda** (18 h, eq 4) to give the species [(tmeda)MgSi(SiMe₃)₃][IB(C₆F₅)₃] (**5-tmeda**) as the product. Compound **5-tmeda** is isolated and fully characterized; however, the nature of the Mg⋯IB(C₆F₅)₃ interaction is difficult to probe through spectroscopic methods and is assigned partly on the basis of comparison with the NMR spectroscopy of **3-tmeda** and **4-tmeda**, partly on the basis of the reaction stoichiometry suggested by the observation of SiMe₄, and partly on the basis of the elemental composition.

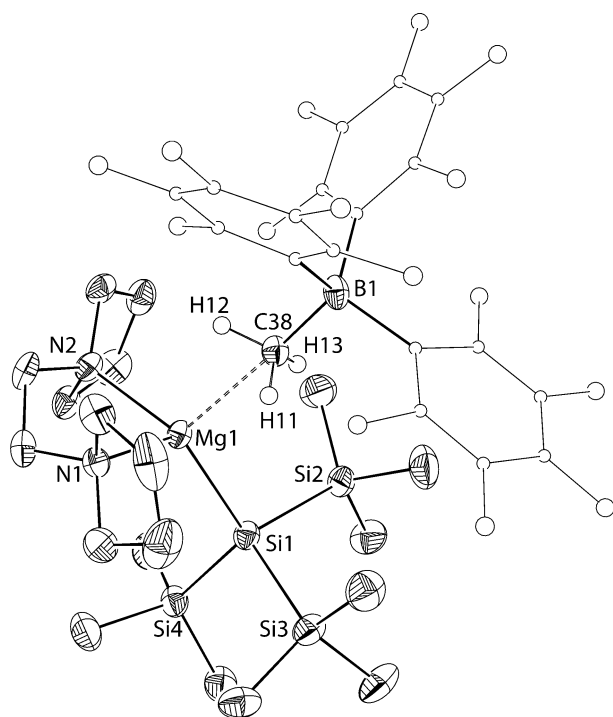


Figure 4. ORTEP diagram of $(dpe)Mg\{Si(SiMe_3)_3\}MeB(C_6F_5)_3$ (**4-dpe**). Ellipsoids are plotted at 35% probability. Hydrogen atoms on the $MeB(C_6F_5)_3$ were located objectively in the Fourier difference map, refined isotropically, and included in the illustration. All other hydrogen atoms were not illustrated for clarity. Fluorine atoms and carbon atoms on $MeB(C_6F_5)_3$ were refined anisotropically and have normal thermal parameters but are depicted using a ball-and-stick representation for clarity. Selected distances (Å): Mg1–Si1, 2.602(2); Mg1–N1, 2.191(3); Mg1–N2, 2.177(3); Mg1–C38, 2.459(4); Mg1–H11, 2.34(3); Mg1–H12, 2.21(3); Mg1–H13, 2.34(3). Selected angles (deg): N1–Mg1–N2, 84.5(1); Si1–Mg1–C38, 109.51; Mg1–C38–B1, 174.1(3).

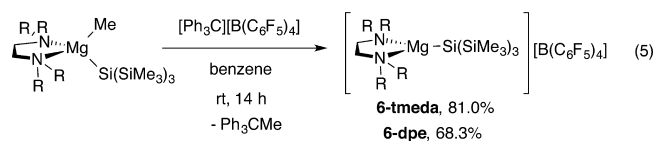


The 1H NMR resonance of the $Si(SiMe_3)_3$ group in **5-tmeda** appeared at 0.36 ppm, which was between the chemical shift for the neutral magnesium iodide (**3-tmeda**) and magnesium methylborate (**4-tmeda**, see Table 1). The ^{11}B NMR spectrum of **5-tmeda** contained a single resonance at -14.3 ppm. **5-tmeda** is an unusual compound, and although it is not crystallographically characterized, a search of the Cambridge Structural Database returned no $IB(C_6F_5)_3$ compounds and few $M-I-B(aryl)_3$ complexes.²³ Interestingly a late metal iodide interaction with a boron center in 5-diphenylboryl-4-diphenylphosphino-thioxanthene coordinated compounds is supported crystallographically, while the ^{11}B NMR chemical shift of $+56$ ppm is similar to the borane ligand ($+65$).²⁴ Bromide and chloride give greater ^{11}B NMR chemical shift differences in this late metal system. The chemical shifts of $\{C_5H_4B(C_6F_5)_2\}-TiCl_3$ (^{11}B NMR, 59.8 ppm) and $\{C_5H_4B(C_6F_5)_2\}CpTiCl_2$ (^{11}B NMR, 4.5 ppm) are also worth noting.²⁵ In contrast, treatment of **4-tmeda** with other electrophiles, such as MeI and MeOTf, provides only $HSi(SiMe_3)_3$; neither $MeSi(SiMe_3)_3$ nor ethane were observed in the reactions.

The reactivity of the Mg–Si bond in **4-tmeda** was probed in silyl group transfer reactions. Reactions of **4-tmeda** and Cp_2MCl_2 ($M = Zr, Hf$) in benzene or bromobenzene- d_5 instantaneously produce a mixture of one new Cp_2M -containing product and one **tmeda**-containing species. The Cp_2M -containing species is tentatively assigned as $Cp_2MClMeB(C_6F_5)_3$ because other conceivable products such as $Cp_2M\{Si(SiMe_3)_3\}Cl$,^{6a} $Cp_2M\{Si(SiMe_3)_3\}Me$,^{6a} $Cp_2M\{Si(SiMe_3)_3\}MeB(C_6F_5)_3$,^{12c} and Cp_2MMeCl are ruled out by comparison with 1H NMR and ^{29}Si NMR spectra of authentic samples or literature values. The magnesium-containing species is postulated to be $(tmeda)Mg\{Si(SiMe_3)_3\}Cl$. Attempts to independently prepare this compound were unsuccessful because reaction of **2-tmeda** and Me_3SiCl gives $Si(SiMe_3)_4$ rather than $SiMe_4$. Further support for this assignment comes from the ^{29}Si NMR chemical shift of the $MSi(SiMe_3)_3$ product of -166.4 ppm, which is similar to the upfield value for **3-tmeda** (-168.9) and all the other magnesium silyls, rather than the (relatively) downfield value for zirconocene and hafnocene silyl compounds (e.g., -84 ppm for $Cp_2Hf\{Si(SiMe_3)_3\}Me$).^{12c} Thus, silyl group transfer to Cp_2MCl_2 is not effective with **4-tmeda**. Despite this, given possible pathways of electron transfer and reduction versus group transfer for interaction of magnesium silyls and transition metal centers, the less reducing character of **4-tmeda** and other cationic organomagnesium compounds may prove valuable as reagents for transmetalations where Grignard reagents give reduction.

In addition, the decreased reactivity of the cationic magnesium silyls contrasts the results comparing group 4 neutral and silyl cationic species in which the latter show enhanced reactivity. Cationic zirconium and hafnium silyl compounds are more reactive in σ -bond metathesis reactions with silanes and with C–H bonds of arenes than their neutral counterparts,^{12b,c,26,27} and dehydropolymerization of organosilanes is sometimes more effective with cationic group 4 catalysts.²⁸

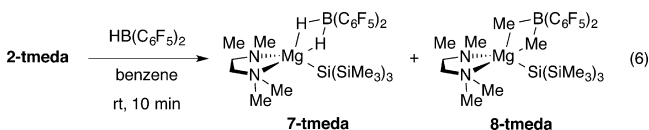
4. Reactions of 2-tmeda or 2-dpe with $[Ph_3C][B(C_6F_5)_4]$. We also examined the reaction of the magnesium silyl compounds with $[Ph_3C][B(C_6F_5)_4]$ in an effort to generate cationic Mg silyl complexes containing a less coordinating anion. The reactions of **2-tmeda** or **2-dpe** and $[Ph_3C][B(C_6F_5)_4]$ in benzene give deep brown oily residues that solidify after benzene and pentane washes. The benzene-soluble materials contained Ph_3CMe , providing evidence of methine group abstraction (eq 5).



The 1H NMR chemical shifts of the $SiMe_3$ moiety in **6-tmeda** and **6-dpe** (0.28 ppm and 0.30 ppm, respectively) were upfield compared to the neutral silyl methyl species, and this follows the tendency observed for the $SiMe_3$ resonances in **4-tmeda** and **4-dpe**, which were also upfield (see Table 1) versus the same precursors. As in **4-tmeda**, the NMe_2 and NCH_2 1H NMR resonances appeared as two singlets that indicated a pseudo- C_{2v} symmetry with no interaction, or at best a highly labile $Mg \cdots [B(C_6F_5)_4]$ interaction. In addition, the ^{19}F NMR spectrum contained three sets of resonances assigned to *meta*, *para*, and *ortho* fluorine atoms on the $B(C_6F_5)_4$ anion. The solubility properties and general

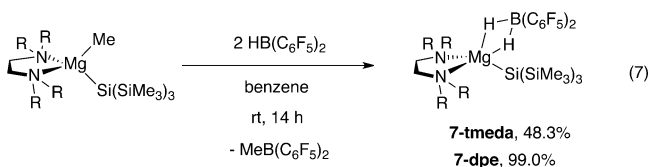
spectroscopic trends thus suggest the products as [(tmeda)-MgSi(SiMe₃)₃]⁺ (**6-tmeda**) and [(dpe)MgSi(SiMe₃)₃]⁺ (**6-dpe**).

5. Reactions of Magnesium Silyl Compounds and HB(C₆F₅)₂. The reactive site in the interaction of **2-tmeda** and electrophiles depends on size (MeX vs Me₃SiX) and leaving groups (I vs OTf). On the basis of those results, a smaller and weaker Lewis acid, such as HB(C₆F₅)₂, could potentially interact with the silyl group. However as in the B(C₆F₅)₃ chemistry, the reaction of HB(C₆F₅)₂ and **2-tmeda** in benzene-d₆ instead involves the magnesium methyl group to afford a 1:1 mixture of (tmeda)MgSi(SiMe₃)₃(μ-H)₂B(C₆F₅)₂ (**7-tmeda**) and (tmeda)MgSi(SiMe₃)₃(μ-Me)₂B(C₆F₅)₂ (**8-tmeda**) (eq 6).



Two Si(SiMe₃)₃ resonances were observed in the ¹H NMR spectrum, which suggested that two Mg silyl species were present in the reaction mixture. A broad quartet at 2.24 ppm and a broad singlet at 0.77 ppm were assigned to H₂B(C₆F₅)₂ and Me₂B(C₆F₅)₂, respectively. The ¹¹B NMR spectrum contained a broad singlet (δ -12.9) and a triplet (δ -28.6, ¹J_{BH} = 69.6 Hz) that were assigned to dimethylborate Me₂B(C₆F₅)₂ and dihydroborate H₂B(C₆F₅)₂ groups, respectively. The methylhydridoborate complex (tmeda)MgSi(SiMe₃)₃(μ-H)(μ-Me)B(C₆F₅)₂, which would be readily distinguished from H₂B(C₆F₅)₂ and Me₂B(C₆F₅)₂ compounds by ¹¹B NMR spectroscopy, was not observed. For comparison, a bis(dihydroborate) adduct Cp₂Zr{(μ-H)₂B(C₆F₅)₂}₂ is prepared from Cp₂ZrMe₂ and 4 equiv of HB(C₆F₅)₂.²⁹ Interestingly, the ¹¹B NMR shift in **7-tmeda** is 15.6 ppm upfield from the signal for Cp₂Zr{(μ-H)₂B(C₆F₅)₂}₂ (-12.9 ppm, ¹J_{BH} = 64 Hz).³⁰

Addition of HB(C₆F₅)₂ to the mixture of **7-tmeda** and **8-tmeda** results in quantitative and rapid conversion to **7-tmeda** and MeB(C₆F₅)₂; the latter species was identified by comparison of ¹¹B NMR and ¹⁹F NMR chemical shifts to literature values.³¹ The compound **7-tmeda**, as well as the dpe analogue (dpe)MgSi(SiMe₃)₃(μ-H)₂B(C₆F₅)₂ (**7-dpe**), are also prepared directly from 2 equiv of HB(C₆F₅)₂ and **2-tmeda** or **2-dpe** in good yield (eq 7).



The ¹H NMR spectrum of the isolated dihydroborate species **7-tmeda** contained two singlets at 1.84 and 1.69 ppm assigned to diastereotopic NMe₂ groups as well as broad resonances at 1.55–1.40 and 1.38–1.25 ppm for the NCH₂ group. The ¹H NMR spectral splitting pattern suggests a pseudotetrahedral Mg center. Furthermore, a broad quartet (2.23 ppm, ¹J_{BH} = 72.1 Hz) and a sharp singlet (0.28 ppm) were assigned to BH₂ and SiMe₃ groups, respectively. One ν_{BH} band (2268 cm⁻¹) was detected in the IR spectrum of **7-tmeda** (KBr), while the spectrum from **7-dpe** contained two bands at

2361 and 2333 cm⁻¹. For comparison, the IR spectrum of [Li(Et₂O)][H₂B(C₆F₅)₂] has two bands at 2380 and 2318 cm⁻¹ assigned to ν_{BH} stretches,³² while the spectra for Cp₂Ti(μ-H)₂B(C₆F₅)₂ (2073, 2008, 1367 cm⁻¹)³² and Cp₂Zr{(μ-H)₂B(C₆F₅)₂}₂ (2184, 2110, 2028 cm⁻¹) are more complex.³⁰ Addition of PMe₃ to Cp₂Ti(μ-H)₂B(C₆F₅)₂ shifts the ν_{BH} to higher energy IR bands at 2361 and 2314 cm⁻¹.³² Thus, comparison of blue-shifted ν_{BH} for **7-dpe** to **7-tmeda** suggests that dpe is a better donor than tmeda in this magnesium system.

The solid-state structure, which is consistent with the solution-phase spectral data, shows that **7-dpe** is a contact ion-pair that contains a Mg(μ-H)₂B(C₆F₅)₂ bridging structure (see the ORTEP diagram in Figure 5). The Mg–Si distance of

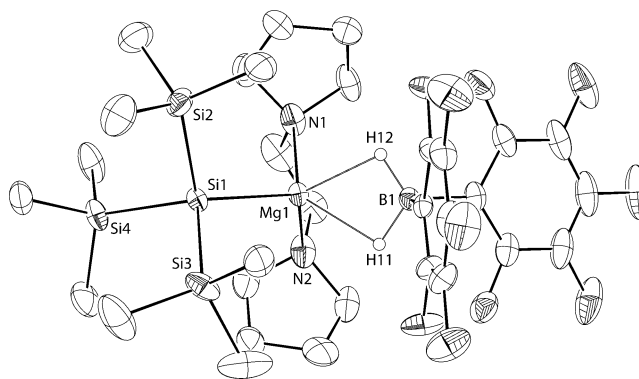


Figure 5. ORTEP diagram of **7-dpe**. Ellipsoids are plotted at 35% probability. Hydrogen atoms on the H₂B(C₆F₅)₂ were located objectively in the Fourier difference map, refined isotropically, and included in the plot. All other hydrogen atoms were not included in the plot. Selected distances (Å): Mg1–Si1, 2.648(1); Mg1–N1, 2.217(4); Mg1–N2, 2.187(4); Mg1–H11, 2.09(4); Mg1–H12, 2.05(4); B1–H11, 1.17(4); B1–H12, 1.12(4). Selected angles (deg): N1–Mg1–N2, 82.9(2); Si1–Mg1–B1, 118.1(1).

2.648(1) Å is ca. 0.05 Å longer than the distance in **4-tmeda** but identical to neutral **2-tmeda** (Table 2). The Mg–N bonds are shorter by ca. 0.03 Å in the dihydroborate compounds than the neutral compounds. The Mg–H distances are 2.09(4) and 2.05(4) Å, and these are within the sum of van der Waals radii of Mg and H (Σ_{VDW}(MgH) = 2.82 Å). The Mg–B distance of 2.507(4) Å in **7-dpe** is on the high end value of those in polymeric [Mg(μ-κ²-BH₄)₂]_n (Mg–B, 2.31(3)–2.53(4)).³³ The B–H bond distances are identical within error to those of Cp₂Ti(μ-H)₂B(C₆F₅)₂, and the H–B–H angle (109.0(3)°) for **7-dpe** falls between the values for [Li(Et₂O)]-[B(C₆F₅)₂H₂]₂ and Cp₂Ti(μ-H)₂B(C₆F₅)₂, which are 111.6(5)° and 100.8(7)°.³²

CONCLUSION

Studies of neutral, zwitterionic, and cationic d⁰ transition metal alkyl compounds (particularly of Group 4) have provided an often accepted trend that increased charge results in enhanced reactivity in olefin insertion and σ-bond metathesis. The zwitterionic and cationic magnesium silyl compounds reported here provide the first opportunity for such a comparison of main group silyl compounds. Notably, the conclusion is that cationic magnesium silyl compounds are less reactive than corresponding neutral silyl alkyl compounds based on transmetalation reactions with a few silicon-based electrophiles and group 4 halides. In this context, we briefly comment on the

air-sensitivity of the magnesium silyls: reactions of O₂ and the neutral or cationic compounds described here do not provide isolable products. However, the qualitative reactivity is striking. Reaction of neutral **2-tmeda** and O₂ (less than 1 atm) occurs vigorously at 0 °C as a frozen benzene-*d*₆ solution melted and ignites to produce a flame in the NMR tube reaction vessel. In contrast, zwitterionic **4-tmeda** and O₂ react under these conditions without catching fire to only slightly warm the NMR tube. In the latter case, broad SiMe₃ signals in the ¹H NMR spectrum were observed, while no components could be assigned in the spectra of the former reaction. Thus, even in kinetically vigorous reactions of magnesium species, the cationic complex shows subdued reactivity in comparison to the neutral precursor.

The current study of a series of neutral, zwitterionic, and cationic compounds allows some spectroscopic comparisons, and we noted above that the SiMe₃ ¹H NMR resonances for the cationic and zwitterionic compounds are upfield versus the silyl group in the methyl compound. In addition, the ²⁹Si NMR chemical shift of the silicon bonded to magnesium moves downfield as the apparent charge separation in the other X-type ligand is increased (Table 1).^{9,10} Thus, the trend [(**tmeda**)-MgSi(SiMe₃)₃][B(C₆F₅)₄] (**6-tmeda**) (−163.4 ppm) > (**tmeda**)Mg{Si(SiMe₃)₃}MeB(C₆F₅)₃ (**4-tmeda**) (−167.2 ppm) > (**tmeda**)Mg{Si(SiMe₃)₃}(μ-H)₂B(C₆F₅)₂ (**7-tmeda**) (−173.1 ppm) > (**tmeda**)Mg{Si(SiMe₃)₃}Me (**2-tmeda**) (−175.4 ppm) nicely follows the expected degree of cationic character of the magnesium silyl portion of complexes resulting from increased charge separation.

EXPERIMENTAL SECTION

General Procedures. All reactions were performed under a dry argon atmosphere using standard Schlenk techniques or under a nitrogen atmosphere in a glovebox unless otherwise indicated. Dry, oxygen-free solvents were used throughout. Benzene, toluene, pentane, and tetrahydrofuran were degassed by sparging with nitrogen, filtered through activated alumina columns, and stored under N₂. Benzene-*d*₆ and THF-*d*₈ were vacuum transferred from Na/K alloy and stored under N₂ in the glovebox. (**tmeda**)Mg(Me)Br,¹⁴ KSi(SiMe₃)₃,¹⁰ B(C₆F₅)₃,³⁴ HB(C₆F₅)₂,³⁵ [Ph₃C][B(C₆F₅)₄],³⁶ and **dpe**³⁷ were prepared according to literature procedures, and 3.0 M MeMgBr in diethyl ether was purchased from Aldrich and used as received. ¹H and ¹³C{¹H} NMR spectra were collected on a Bruker DRX-400 or Avance III 600 spectrometer. ²⁹Si{¹H} NMR spectra were recorded using DEPT experiments, and assignments were verified by ¹H COSY, ¹H-¹³C HMQC, ¹H-¹³C HMBC, ¹H-¹¹B HMBC, and ¹H-²⁹Si HMBC experiments. Elemental analysis was performed using a Perkin-Elmer 2400 Series II CHN/S in the Iowa State Chemical Instrumentation Facility.

(tmeda)Mg{Si(SiMe₃)₃}Me (2-tmeda). (**tmeda**)Mg(Me)Br (0.269 g, 1.14 mmol) and KSi(SiMe₃)₃ (0.328 g, 1.14 mmol) were dissolved in benzene (10 mL), and the mixture was allowed to stir for 4 h at room temperature. The volatile materials were evaporated under reduced pressure, and the resulting residue was extracted with pentane (3 × 5 mL). The pentane solution was concentrated and cooled to −30 °C to yield **2-tmeda** (0.250 g, 0.620 mmol, 54.4%) as colorless block-like crystals. ¹H NMR (benzene-*d*₆, 600 MHz, 25 °C): δ 1.94 (s, 6 H, NMe), 1.79 (s, 6 H, NMe), 1.56 (s, 4 H, CH₂), 0.51 (s, 27 H, SiMe₃), −1.03 (s, 3 H, CH₃). ¹³C{¹H} NMR (benzene-*d*₆, 150 MHz, 25 °C): δ 56.2 (NCH₂), 47.7 (NMe), 46.6 (NMe), 6.02 (SiMe₃), −11.4 (MgMe). ²⁹Si{¹H} NMR (benzene-*d*₆, 119.3 MHz, 25 °C): δ −7.1 (SiMe₃), −175.4 (Si(SiMe₃)₃). IR (KBr, cm^{−1}): 2994 m, 2944 s, 2887 s, 2852 s, 2806 m, 2778 m, 1465 s, 1288 w, 1236 s, 1027 m, 948 m, 834 s, 677 m. Anal. Calcd for C₁₆H₄₆MgN₂Si₄: C, 47.66; H, 11.50; N, 6.95. Found: C, 47.77; H, 11.51; N, 6.85. Mp 179–180 °C.

(dpe)MgMeBr (1-dpe). 1,2-*N,N*-Dipyrrolideneylethane (1.52 g, 9.01 mmol) and 20 mL of diethyl ether were placed in a 100 mL Schlenk flask. In a second Schlenk flask, 3.0 M MgMeBr (2.70 mL, 8.10 mmol) was diluted with 40 mL of diethyl ether. The 1,2-*N,N*-dipyrrolideneylethane solution was added dropwise to the methyl Grignard solution. A white precipitate formed upon addition, and the resulting mixture was allowed to stir for 1 h. The white solid was isolated by filtration and dried under vacuum to yield **1-dpe** (1.94 g, 6.73 mmol, 83.1%). ¹H NMR (THF-*d*₈, 600 MHz, 25 °C): δ 2.71 (s br, 8 H, NCH₂(CH₂)₂CH₂), 2.69 (s, 4 H, NCH₂), 1.81 (m, 8 H, NCH₂(CH₂)₂CH₂), −1.65 (s, 3 H, MgMe). ¹³C{¹H} NMR (THF-*d*₈, 150 MHz, 25 °C): δ 55.7 (NCH₂(CH₂)₂CH₂ + NCH₂), 24.0 (NCH₂(CH₂)₂CH₂), −17.3 (MgMe). IR (KBr, cm^{−1}): 2973 s, 2858 s, 2781 m, 1462 s, 1374 w, 1334 w, 1307 w, 1266 w, 1101 m, 1968 m, 945 m, 863 w. Anal. Calcd for C₁₁H₂₃BrMgN₂: C, 45.95; H, 8.06; N, 9.74. Found: C, 45.00; H, 7.74; N, 9.40. Mp 196–197 °C.

(dpe)Mg{Si(SiMe₃)₃}Me (2-dpe). **2-dpe** was prepared following the procedure for **2-tmeda** with **1-dpe** (0.906 g, 3.15 mmol) and KSi(SiMe₃)₃ (0.904 g, 3.15 mmol) to yield **2-dpe** (0.928 g, 2.04 mmol, 64.7%) as colorless blocky crystals. ¹H NMR (benzene-*d*₆, 400 MHz, 25 °C): δ 3.33–3.23 (m, 2 H, NCH₂(CH₂)₂CH₂), 3.09–2.99 (m, 2 H, NCH₂(CH₂)₂CH₂), 1.93–2.04 (m, 2 H, NCH₂), 1.87–1.71 (m, 2 H, NCH₂ + NCH₂(CH₂)₂CH₂), 1.71–1.59 (m, 4 H, NCH₂(CH₂)₂CH₂), 1.44–1.22 (m, 4 H, NCH₂(CH₂)₂CH₂), 0.51 (s, 27 H, SiMe₃), −1.02 (s, 3 H, MgMe). ¹³C{¹H} NMR (benzene-*d*₆, 125 MHz, 25 °C): δ 57.5 (NCH₂(CH₂)₂CH₂), 55.3 (NCH₂(CH₂)₂CH₂), 55.1 (NCH₂), 23.6 (NCH₂(CH₂)₂CH₂), 23.5 (NCH₂(CH₂)₂CH₂), 6.2 (SiMe₃), −11.9 (MgMe). ²⁹Si{¹H} NMR (benzene-*d*₆, 119.3 MHz, 25 °C): δ −7.2 (SiMe₃), −177.0 (Si(SiMe₃)₃). IR (KBr, cm^{−1}): 2957 s, 2886 m, 2776 m, 2051 w, 1462 w, 1389 w, 1336 w, 1293 w, 1235 m, 1095 w, 1057 w, 950 w, 835 m br, 746 w, 676 m. Anal. Calcd for C₂₀H₅₀MgN₂Si₄: C, 52.76; H, 11.07; N, 6.15. Found: C, 52.97; H, 11.31; N, 6.03. Mp 226–233 °C.

(tmeda)Mg{Si(SiMe₃)₃}I (3-tmeda). Trimethylsilyl iodide (93.3 μL, 0.658 mmol) was added to a benzene solution (5 mL) of **2-tmeda** (0.204 g, 0.506 mmol). The mixture was allowed to stir for 30 min. The volatile materials were evaporated under reduced pressure. The residue was dissolved in toluene (2 mL) and cooled to −30 °C to give **3-tmeda** (0.186 g, 0.362 mmol, 71.4%) as colorless crystals. ¹H NMR (benzene-*d*₆, 600 MHz, 25 °C): δ 2.06 (s, 6 H, NMe), 1.88 (s, 6 H, NMe), 1.63–1.67 (m, 2 H, CH₂), 1.43–1.47 (m, 2 H, CH₂), 0.50 (s, 27 H, SiMe₃). ¹³C{¹H} NMR (benzene-*d*₆, 150 MHz, 25 °C): δ 56.0 (NCH₂), 48.9 (NMe₂), 47.2 (NMe₂), 5.84 (SiMe₃). ²⁹Si{¹H} NMR (benzene-*d*₆, 119.3 MHz, 25 °C): δ −7.3 (SiMe₃), −167.9 (Si(SiMe₃)₃). IR (KBr, cm^{−1}): 2994 m, 2956 s, 2891 s, 2810 m, 1465 s, 1287 w, 1260 m, 1238 m, 1023 s br, 948 m, 831 s br, 677 m. Anal. Calcd for C₁₅H₄₃ISi₄N₂Mg: C, 34.98; H, 8.41; N, 5.44. Found: C, 34.79; H, 8.50; N, 5.56. Mp: 204–205 °C.

(dpe)Mg{Si(SiMe₃)₃}I (3-dpe). **3-dpe** was prepared following the procedure for **3-tmeda**, using **2-dpe** (0.120 g, 0.263 mmol) and Me₃SiI (39.2 μL, 0.276 mmol) to yield **3-dpe** (0.136 g, 0.239 mmol, 91.0%) as colorless X-ray quality crystals. ¹H NMR (benzene-*d*₆, 400 MHz, 25 °C): δ 3.54 (m br, 2 H, NCH₂(CH₂)₂CH₂), 3.17 (m br, 2 H, NCH₂(CH₂)₂CH₂), 1.82 (s, 4 H, NCH₂), 1.78 (m br, 4 H, NCH₂(CH₂)₂CH₂), 1.29 (m br, 4 H, NCH₂(CH₂)₂CH₂), 0.51 (s, 27 H, SiMe₃). ¹³C{¹H} NMR (benzene-*d*₆, 125 MHz, 25 °C): δ 57.5 (NCH₂(CH₂)₂CH₂), 55.3 (NCH₂(CH₂)₂CH₂), 55.1 (NCH₂), 23.4 (NCH₂(CH₂)₂CH₂), 23.2 (NCH₂(CH₂)₂CH₂), 5.9 (SiMe₃). ²⁹Si{¹H} NMR (benzene-*d*₆, 119.3 MHz, 25 °C): δ −7.4 (SiMe₃), −168.9 (Si(SiMe₃)₃). IR (KBr, cm^{−1}): 2944 m, 2886 m, 1462 m, 1394 w, 1237 s, 1112 w, 1061 w, 945 w, 832 s br, 744 w, 677 m, 622 m. Anal. Calcd for C₁₉H₄₇IN₂MgSi₄: C, 40.24; H, 8.35; N, 4.94. Found: C, 40.14; H, 8.27; N, 5.10. Mp 240–243 °C.

[(tmeda)Mg{Si(SiMe₃)₃}MeB(C₆F₅)₃] (4-tmeda). B(C₆F₅)₃ (0.270 g, 0.521 mmol) was added to a benzene solution (5 mL) of **2-tmeda** (0.200 g, 0.497 mmol) to give a pale yellow solution. The mixture was stirred for 1.5 h. The volatiles were evaporated under reduced pressure to give **4-tmeda** (0.335 g, 0.366 mmol, 73.6%) as a pale yellow solid. ¹H NMR (benzene-*d*₆, 600 MHz, 25 °C): δ 1.66 (s, 12 H, NMe₂), 1.44 (m, 4 H, CH₂), 0.94 (s, 3 H, BMe), 0.175 (s, 27 H,

SiMe₃). ¹³C{¹H} NMR (benzene-*d*₆, 150 MHz, 25 °C): δ 150.3 (br, C₆F₅), 148.7 (br, C₆F₅), 140.2 (br, C₆F₅), 138.7 (br, C₆F₅), 137.0 (br, C₆F₅), 56.1 (NCH₂), 46.6 (NMe₂), 5.1 (SiMe₃), the MeB resonance was not observed. ¹¹B{¹H} NMR (benzene-*d*₆, 125 MHz, 25 °C): δ -14.3. ¹¹B NMR (bromobenzene-*d*₅, 79.5 MHz, 25 °C): δ -15.1. ¹⁹F NMR (benzene-*d*₆, 376 MHz, 25 °C): δ -132.8 (d, ³J_{FF} = 22.9 Hz, 6 F, *o*-F), -161.3 (t, ³J_{FF} = 21.8 Hz, 3 F, *p*-F), -165.3 (t, ³J_{FF} = 18.8 Hz, 6 F, *m*-F). ¹⁹F NMR (bromobenzene-*d*₅, 376 MHz, 25 °C): δ -133.7 (d, ³J_{FF} = 23.3 Hz, 6 F, *o*-F), -161.9 (t, ³J_{FF} = 20.6 Hz, 3 F, *p*-F), -165.7 (t, ³J_{FF} = 20.7 Hz, 6 F, *m*-F). ²⁹Si{¹H} NMR (benzene-*d*₆, 119.3 MHz, 25 °C): δ -7.8 (SiMe₃), -167.2 (Si(SiMe₃)₃). IR (KBr, cm⁻¹): 2954 m, 2896 m, 1644 m, 1513 s, 1459 s br, 1244 m br, 1087 s, 977 s, 836 s br, 757 m. Anal. Calcd for C₃₉H₄₆BF₁₅MgN₂Si₄: C, 44.62; H, 5.07; N, 3.06. Found: C, 44.84; H, 4.90; N, 3.07. Mp 130–133 °C.

[(dpe)Mg{Si(SiMe₃)₃}MeB(C₆F₅)₃ (4-dpe). B(C₆F₅)₃ (0.194 g, 0.379 mmol) was added to a benzene solution (5 mL) of **2-dpe** (0.173 g, 0.380 mmol) to give a pale yellow solution. The mixture was stirred for 1.5 h. The volatiles were evaporated under reduced pressure. The oily residue was washed with pentane (2 × 5 mL) and dried under reduced pressure to give **4-dpe** (0.311 g, 0.321 mmol, 84.6%) as a pale yellow solid. ¹H NMR (bromobenzene-*d*₅, 400 MHz, 25 °C): δ 3.07 (m br, 4 H, NCH₂(CH₂)₂CH₂), 2.35 (s, 4 H, NCH₂), 2.29 (m, 4 H, NCH₂(CH₂)₂CH₂), 1.65 (m, 4 H, NCH₂(CH₂)₂CH₂), 1.54 (m, 4 H, NCH₂(CH₂)₂CH₂), 1.03 (s br, 3 H, MeB(C₆F₅)₃), 0.24 (s, 27 H, SiMe₃). ¹³C{¹H} NMR (bromobenzene-*d*₅, 125 MHz, 25 °C): δ 148.5 (br, C₆F₅), 146.1 (br, C₆F₅), 138.6 (br, C₆F₅), 137.0 (br, C₆F₅), 136.1 (br, C₆F₅), 134.5 (br, C₆F₅), 54.0 (NCH₂(CH₂)₂CH₂), 53.4 (NCH₂), 21.4 (NCH₂(CH₂)₂CH₂), 10.8 (br, BMe), 3.5 (SiMe₃). ¹¹B NMR (bromobenzene-*d*₅, 79.5 MHz, 25 °C): δ -14.8. ¹⁹F NMR (bromobenzene-*d*₅, 376 MHz, 25 °C): δ -132.9 (br), -165.1 (br), -167.9 (br). ²⁹Si{¹H} NMR (bromobenzene-*d*₅, 119.3 MHz, 25 °C): δ -7.7 (SiMe₃), -168.7 (Si(SiMe₃)₃). IR (KBr, cm⁻¹): 2960 m, 2890 m, 2811 w, 1642 m, 1514 s, 1460 s, 1379 w, 1261 m, 1244 m, 1087 s, 973 s, 835 s, 803 m, 758 w, 736 w, 648 m. Anal. Calcd for C₃₈H₅₀BF₁₅MgN₂Si₄: C, 47.12; H, 5.21; N, 2.90. Found: C, 47.36; H, 4.71; N, 2.87. Mp 71–72 °C.

(tmeda)Mg{Si(SiMe₃)₃}B(C₆F₅)₃ (5-tmeda). Me₃SiI (12.5 μL, 0.088 mmol) was added to a benzene solution (5 mL) of **4-tmeda** (0.079 g, 0.087 mmol) at room temperature, and the mixture was stirred for 17 h. The volatile materials of the pale yellow reaction mixture was evaporated to dryness to yield **5-tmeda** (0.071 g, 0.069 mmol, 80.1%) as a white solid. ¹H NMR (bromobenzene-*d*₅, 400 MHz, 25 °C): δ 2.32 (s br, 12 H, NMe₂), 2.23 (s br, 4 H, CH₂), 0.36 (s, 27 H, SiMe₃). ¹³C{¹H} NMR (bromobenzene-*d*₅, 150 MHz, 25 °C): δ 148.7 (br, C₆F₅), 146.3 (br, C₆F₅), 136.7 (br, C₆F₅), 134.2 (br, C₆F₅), 54.7 (NCH₂), 46.1 (NMe₂), 4.0 (SiMe₃). ²⁹Si{¹H} NMR (bromobenzene-*d*₅, 119.3 MHz, 25 °C): δ -7.6 (SiMe₃), -165.0 (Si(SiMe₃)₃). ¹¹B{¹H} NMR (bromobenzene-*d*₅, 125 MHz, 25 °C): δ -14.3. ¹⁹F NMR (bromobenzene-*d*₅, 376 MHz, 25 °C): δ -131.5 (d, t, ³J_{FF} = 20.3 Hz, 6 F, *o*-F), -163.3 (t, ³J_{FF} = 21.1 Hz, 3 F, *p*-F), -166.0 (t, ³J_{FF} = 19.6 Hz, 6 F, *m*-F). Anal. Calcd for C₃₃H₄₃BF₁₅IMgN₂Si₄: C, 38.59; H, 4.22; N, 2.73. Found: C, 38.52; H, 3.97; N, 2.83.

[(tmeda)MgSi(SiMe₃)₃][B(C₆F₅)₄] (6-tmeda). [Ph₃C][B(C₆F₅)₄] (0.250 g, 0.271 mmol) was added to a benzene solution of **2-tmeda** (0.104 g, 0.258 mmol). The reaction mixture was stirred overnight, and an oily residue precipitated from benzene. The benzene solvent (top layer) was decanted from the precipitate. The oily residue was washed with benzene (3 × 5 mL) and pentane (3 × 5 mL) to remove the Ph₃CMe byproduct. The remaining material was dried under reduced pressure to give **6-tmeda** (0.223 g, 0.209 mmol, 81.0%) as a light brown solid. ¹H NMR (bromobenzene-*d*₅, 400 MHz, 25 °C): δ 2.20 (s br, 4 H, CH₂), 2.12 (s br, 12 H, NMe), 0.28 (s, 27 H, SiMe₃). ¹³C{¹H} NMR (bromobenzene-*d*₅, 150 MHz, 25 °C): δ 148.6 (br, C₆F₅), 146.2 (br, C₆F₅), 138.5 (br, C₆F₅), 136.7 (br, C₆F₅), 136.0 (br, C₆F₅), 134.3 (br, C₆F₅), 54.5 (NCH₂), 44.4 (NCH₂), 3.6 (SiMe₃). ¹¹B{¹H} NMR (bromobenzene-*d*₅, 125 MHz, 25 °C): δ -15.9. ¹⁹F NMR (bromobenzene-*d*₅, 376 MHz, 25 °C): δ -131.5 (s br, 8 F, *o*-F), -160.9 (t, ³J_{FF} = 20.7 Hz, 4 F, *p*-F), -165.5 (s br, 8 F, *m*-F). ²⁹Si{¹H} NMR (bromobenzene-*d*₅, 119.3 MHz, 25 °C): δ -7.9 (SiMe₃), -163.4 (Si(SiMe₃)₃). IR (KBr, cm⁻¹): 2951 m, 2895 w, 2181 w, 1644

s, 1515 s, 1464 s br, 1374 m, 1278 s, 1244 m, 1091 s br, 980 s br, 834 s br, 769 m, 756 m, 684 s. Anal. Calcd for C₃₉H₄₃BF₂₀MgN₂Si₄: C, 43.89; H, 4.06; N, 2.62. Found: C, 43.93; H, 3.84; N, 2.62. Mp 103–105 °C.

[(dpe)MgSi(SiMe₃)₃][B(C₆F₅)₄] (6-dpe). The procedure for **6-tmeda** was modified, using **2-dpe** (0.101 g, 0.223 mmol) and [Ph₃C][B(C₆F₅)₄] (0.216 g, 0.234 mmol) to yield **6-dpe** (0.170 g, 0.152 mmol, 68.3%) as a light brown solid. ¹H NMR (bromobenzene-*d*₅, 400 MHz, 25 °C): δ 3.09–2.85 (m br, 4 H, NCH₂(CH₂)₂CH₂), 2.60–2.20 (m br, 8 H, CH₂NCH₂(CH₂)₂CH₂), 1.69 (s br, 8 H, NCH₂(CH₂)₂CH₂), 0.30 (s, 27 H, SiMe₃). ¹³C{¹H} NMR (bromobenzene-*d*₅, 150 MHz, 25 °C): δ 144.6 (br, C₆F₅), 142.2 (br, C₆F₅), 134.4 (br, C₆F₅), 132.7 (br, C₆F₅), 132.0 (br, C₆F₅), 130.2 (br, C₆F₅), 49.8 (NCH₂(CH₂)₂CH₂), 49.4 (NCH₂(CH₂)₂CH₂), 49.2 (NCH₂), 49.1 (NCH₂), 17.5 (NCH₂(CH₂)₂CH₂), 17.4 (NCH₂(CH₂)₂CH₂), -0.3 (SiMe₃). ¹¹B{¹H} NMR (bromobenzene-*d*₅, 125 MHz, 25 °C): δ -15.9. ¹⁹F NMR (bromobenzene-*d*₅, 376 MHz, 25 °C): δ -131.7 (d, ³J_{FF} = 9.4 Hz, 8 F, *o*-F), -161.3 (t, ³J_{FF} = 20.7 Hz, 4 F, *p*-F), -165.6 (t, ³J_{FF} = 19.2 Hz, 8 F, *m*-F). ²⁹Si{¹H} NMR (bromobenzene-*d*₅, 119.3 MHz, 25 °C): δ -7.9 (SiMe₃), -170.8 (Si(SiMe₃)₃). IR (KBr, cm⁻¹): 3092 w, 3072 w, 3037 w, 2952 s, 2891 s, 2622 vw, 2596 vw, 2551 vw, 2331 vw, 2177 w, 2088 vw, 2046 vw, 1966 vw, 1825 vw, 1643 s, 1515 s, 1464 s, 1277 s, 1243 s, 1091 s, 1037 s, 980 s, 940 s, 904 s, 834 s, 684 s, 661 s. Anal. Calcd for C₄₃H₄₇BF₂₀MgN₂Si₄: C, 46.14; H, 4.23; N, 2.50. Found: C, 46.29; H, 4.01; N, 2.38. Mp 70–73 °C.

(tmeda)Mg{Si(SiMe₃)₃}(μ-H)₂B(C₆F₅)₂ (7-tmeda). HB(C₆F₅)₂ (0.293 g, 0.271 mmol) was added to a benzene solution of **2-tmeda** (0.123 g, 0.258 mmol) at room temperature. The mixture was stirred for 30 min to provide a homogeneous and colorless solution. The volatile materials were evaporated under reduced pressure to dryness, washed with pentane (2 × 5 mL), and dried under vacuum to yield **7-tmeda** (0.137 g, 0.186 mmol, 52.5%) as a pale white solid. ¹H NMR (benzene-*d*₆, 400 MHz, 25 °C): δ 2.23 (q, ¹J_{BH} = 72.1 Hz, 2 H, BH₂), 1.84 (s, 6 H, NMe), 1.69 (s, 6 H, NMe), 1.55–1.40 (m br, 2 H, NCH₂), 1.38–1.25 (m br, 2 H, NCH₂), 0.28 (s, 27 H, SiMe₃). ¹³C{¹H} NMR (benzene-*d*₆, 150 MHz, 25 °C): δ 149.8 (br, C₆F₅), 147.4 (br, C₆F₅), 141.7 (br, C₆F₅), 139.2 (br, C₆F₅), 136.8 (br, C₆F₅), 56.4 (NCH₂), 47.9 (NMe), 46.5 (NMe), 5.4 (SiMe₃). ¹¹B{¹H} NMR (benzene-*d*₆, 125 MHz, 25 °C): δ -28.5 (t, ¹J_{BH} = 72.1 Hz). ¹⁹F NMR (benzene-*d*₆, 376 MHz, 25 °C): δ -132.7 (d, ³J_{FF} = 21.8 Hz, 4 F, *o*-F), -161.6 (s br, 2 F, *p*-F), -165.4 (s br, 4 F, *m*-F). ²⁹Si{¹H} NMR (benzene-*d*₆, 119.3 MHz, 25 °C): δ -7.7 (SiMe₃), -173.1 (Si(SiMe₃)₃). IR (KBr, cm⁻¹): 2959 m, 2894 w, 2855 w, 2268 w br (ν_{BH}), 1645 m, 1512 s, 1469 s br, 1286 w, 1262 w, 1293 w, 1109 m, 1089 m, 1023 m, 972 m, 832 m, 796 m, 682 w. Anal. Calcd for C₂₇H₄₅BF₁₀MgN₂Si₄: C, 44.12; H, 6.17; N, 3.81. Found: C, 43.53; H, 6.61; N, 3.66. Mp 195–196 °C.

(dpe)MgSi(SiMe₃)₃(μ-H)₂B(C₆F₅)₂ (7-dpe). **7-dpe** was prepared following the procedure for **7-tmeda** with the substitution of **2-dpe**. **2-dpe** (0.057 g, 0.125 mmol) and HB(C₆F₅)₂ (0.089 g, 0.257 mmol) react to give **7-dpe** as a pale white solid in excellent isolated yield (0.098 g, 0.124 mmol, 99.0%). ¹H NMR (benzene-*d*₆, 400 MHz, 25 °C): δ 3.10 (m, 2 H, NCH₂(CH₂)₂CH₂), 2.93 (m, 2 H, NCH₂(CH₂)₂CH₂), 2.31 (q, ¹J_{BH} = 72.4 Hz, 2 H, BH₂), 1.82 (m, 2 H, NCH₂(CH₂)₂CH₂), 1.73 (m, 4 H, NCH₂), 1.59 (m br, 4 H, NCH₂(CH₂)₂CH₂), 1.48 (m, 2 H, NCH₂(CH₂)₂CH₂), 1.21 (m br, 4 H, NCH₂(CH₂)₂CH₂), 0.30 (s, 27 H, SiMe₃). ¹³C NMR (benzene-*d*₆, 125 MHz, 25 °C): δ 149.8 (br, C₆F₅), 147.4 (br, C₆F₅), 139.2 (br, C₆F₅), 136.8 (br, C₆F₅), 56.1 (NCH₂(CH₂)₂CH₂), 55.9 (NCH₂(CH₂)₂CH₂), 54.9 (NCH₂), 23.2 (NCH₂(CH₂)₂CH₂), 22.9 (NCH₂(CH₂)₂CH₂), 5.5 (SiMe₃). ²⁹Si{¹H} NMR (benzene-*d*₆, 119.3 MHz, 25 °C): δ -7.6 (SiMe₃), -173.1 (Si(SiMe₃)₃). ¹¹B{¹H} NMR (benzene-*d*₆, 125 MHz, 25 °C): δ -29.5 (t, ¹J_{BH} = 72.5 Hz). ¹⁹F NMR (benzene-*d*₆, 376 MHz, 25 °C): δ -130.0 (s br, 4 F, *o*-F), -159.0 (t, ³J_{FF} = 19.9 Hz, 2 F, *p*-F), -163.7 (t, ³J_{FF} = 17.7 Hz, 4 F, *m*-F). IR (KBr, cm⁻¹): 2956 m, 2919 m, 2851 m, 2361 vw (ν_{BH}), 2333 vw br (ν_{BH}), 1642 s, 1514 s, 1460 s, 1379 w, 1261 m, 1244 m, 1087 s, 973 s, 835 s, 803 m, 736 w, 684 w, 647 w. Anal. Calcd for C₃₁H₄₉BF₁₀MgN₂Si₄: C, 47.30; H, 6.27; N, 3.56. Found: C, 46.80; H, 5.96; N, 3.46. Mp 193–196 °C.

■ ASSOCIATED CONTENT

■ Supporting Information

Crystallographic information files (CIF format) for the compounds **2-tmeda**, **3-dpe**, **4-tmeda**, **4-dpe**, and **7-dpe**. This material is available free of charge via the Internet at <http://pubs.acs.org>.

■ AUTHOR INFORMATION

Corresponding Author

*E-mail: sadow@iastate.edu.

Notes

The authors declare no competing financial interest.

■ ACKNOWLEDGMENTS

The authors gratefully thank the National Science Foundation (CHE-0955635, CRIF-0946687, and MRI-1040098) for financial support. The Office of Workforce Development for Teachers and Scientists through the Summer Undergraduate Laboratory Internship Program through the Ames Laboratory is thanked for support (B.M.U.). The Ames Laboratory is operated for the U.S. Department of Energy by Iowa State University under Contract No. DE-AC02-07CH11358. The work was carried out in the facilities of the Ames Laboratory and the Chemistry Department at Iowa State University.

■ REFERENCES

- (1) Tilley, T. D. In *The Silicon–Heteroatom Bond*; Patai, S., Rappaport, Z., Eds.; Wiley: Chichester, 1991.
- (2) Marschner, C. *Eur. J. Inorg. Chem.* **1998**, 221–226.
- (3) Roddick, D. M.; Heyn, R. H.; Tilley, T. D. *Organometallics* **1989**, *8*, 324–330.
- (4) (a) Jiang, Q.; Pestana, D. C.; Carroll, P. J.; Berry, D. H. *Organometallics* **1994**, *13*, 3679–3691. (b) Koga, N.; Morokuma, K. *J. Am. Chem. Soc.* **1993**, *115*, 6883–6892. (c) Yu, X.; Morton, L. A.; Xue, Z.-L. *Organometallics* **2004**, *23*, 2210–2224.
- (5) King, W. A.; Marks, T. J. *Inorg. Chim. Acta* **1995**, *229*, 343–354.
- (6) (a) Campion, B. K.; Falk, J.; Tilley, T. D. *J. Am. Chem. Soc.* **1987**, *109*, 2049–2056. (b) Woo, H.-G.; Heyn, R. H.; Tilley, T. D. *J. Am. Chem. Soc.* **1992**, *114*, 5698–5707.
- (7) Campion, B. K.; Heyn, R. H.; Tilley, T. D. *Organometallics* **1993**, *12*, 2584–2590.
- (8) Corey, J. Y. *Chem. Rev.* **2011**, *111*, 863–1071.
- (9) Farwell, J. D.; Lappert, M. F.; Marschner, C.; Strissel, C.; Tilley, T. D. *J. Organomet. Chem.* **2000**, *603*, 185–188.
- (10) Gaderbauer, W.; Zirngast, M.; Baumgartner, J.; Marschner, C.; Tilley, T. D. *Organometallics* **2006**, *25*, 2599–2606.
- (11) (a) Fabicon, R. M.; Pajerski, A. D.; Richey, H. G., Jr. *J. Am. Chem. Soc.* **1993**, *115*, 9333–9334. (b) Pajerski, A. D.; Squiller, E. P.; Parvez, M.; Whittle, R. R.; Richey, H. G., Jr. *Organometallics* **2005**, *24*, 809–814. (c) Ireland, B. J.; Wheaton, C. A.; Hayes, P. G. *Organometallics* **2010**, *29*, 1079–1084. (d) Sarazin, Y.; Schormann, M.; Bochmann, M. *Organometallics* **2004**, *23*, 3296–3302. (e) Layfield, R. A.; Bullock, T. H.; García, F.; Humphrey, S. M.; Schüler, P. *Chem. Commun.* **2006**, 2039–2041. (f) Sarazin, Y.; Poirier, V.; Roisnel, T.; Carpentier, J.-F. *Eur. J. Inorg. Chem.* **2010**, 3423–3428. (g) Brignou, P.; Guillaume, S. M.; Roisnel, T.; Bourissou, D.; Carpentier, J.-F. *Chem.—Eur. J.* **2012**, *18*, 9360–9370. (h) Sarazin, Y.; Liu, B.; Roisnel, T.; Maron, L.; Carpentier, J.-F. *J. Am. Chem. Soc.* **2011**, *133*, 9069–9087.
- (12) (a) Dioumaev, V. K.; Harrod, J. F. *Organometallics* **1994**, *13*, 1548–1550. (b) Jordan, R. F.; Taylor, D. F.; Baenziger, N. C. *Organometallics* **1990**, *9*, 1546–1557. (c) Wu, F.; Jordan, R. F. *Organometallics* **2005**, *24*, 2688–2697. (d) Sadow, A. D.; Tilley, T. D. *J. Am. Chem. Soc.* **2002**, *124*, 6814–6815. (e) Sadow, A. D.; Tilley, T. D. *J. Am. Chem. Soc.* **2003**, *125*, 9462–9475.
- (13) (a) Jordan, R. F.; Bajgur, C. S.; Willett, R.; Scott, B. *J. Am. Chem. Soc.* **1986**, *108*, 7410–7411. (b) Hlatky, G. G.; Turner, H. W.; Eckman, R. R. *J. Am. Chem. Soc.* **1989**, *111*, 2728–2729. (c) Yang, X.; Stern, C. L.; Marks, T. J. *J. Am. Chem. Soc.* **1994**, *116*, 10015–10031.
- (14) Yousef, R. I.; Walfort, B.; Rüffer, T.; Wagner, C.; Schmidt, H.; Herzog, R.; Steinborn, D. *J. Organomet. Chem.* **2004**, *690*, 1178–1191.
- (15) (a) Guzei, I. A.; Wendt, M. *Dalton Trans.* **2006**, 3991–3999. (b) Guzei, I. A.; Wendt, M. *Solid-G*; University of Wisconsin-Madison: Madison, Wisconsin, 2004.
- (16) Camara, J. M.; Petros, R. A.; Norton, J. R. *J. Am. Chem. Soc.* **2011**, *133*, 5263–5273.
- (17) (a) Deck, P. A.; Beswick, C. L.; Marks, T. J. *J. Am. Chem. Soc.* **1998**, *120*, 1772–1784. (b) Beswick, C. L.; Marks, T. J. *J. Am. Chem. Soc.* **2000**, *122*, 10358–10370.
- (18) Hayes, P. G.; Piers, W. E.; Parvez, M. *Organometallics* **2005**, *24*, 1173–1183.
- (19) (a) Horton, A. D.; de With, J.; van der Linden, A. J.; van de Weg, H. *Organometallics* **1996**, *15*, 2672–2674. (b) Horton, A. D.; de With, J. *Organometallics* **1997**, *16*, 5424–5436.
- (20) Pregosin, P. S.; Martínez-Viviente, E.; Kumar, P. G. H. *Dalton Trans.* **2003**, 4007–4014. (b) Valentini, M.; Pregosin, P. S.; Ruegger, H. *Organometallics* **2000**, *19*, 2551–2555.
- (21) Shannon, R. D. *Acta Crystallogr.* **1976**, *A32*, 751–767.
- (22) White, D.; Coville, N. J. *Adv. Organomet. Chem.* **1994**, *36*, 95–158.
- (23) (a) Cowie, B. E.; Emslie, D. J. H.; Jenkins, H. A.; Britten, J. F. *Inorg. Chem.* **2010**, *49*, 4060–4072. (b) Emslie, D. J. H.; Cowie, B. E.; Oakley, S. R.; Huk, N. L.; Jenkins, H. A.; Harrington, L. E.; Britten, J. F. *Dalton Trans.* **2012**, *41*, 3523–3535.
- (24) Emslie, D. J. H.; Blackwell, J. M.; Britten, J. F.; Harrington, L. E. *Organometallics* **2006**, *25*, 2412–2414.
- (25) Lancaster, S. J.; Al-Benna, S.; Thornton-Pett, M.; Bochmann, M. *Organometallics* **2000**, *19*, 1599–1608.
- (26) (a) Sadow, A. D.; Tilley, T. D. *Organometallics* **2001**, *20*, 4457–4459. (b) Sadow, A. D.; Tilley, T. D. *Organometallics* **2003**, *22*, 3577–3585.
- (27) Wu, F.; Jordan, R. F. *Organometallics* **2005**, *24*, 2688–2697.
- (28) (a) Dioumaev, V. K.; Harrod, J. F. *Organometallics* **1994**, *13*, 1548–1550. (b) Dioumaev, V. K.; Harrod, J. F. *Organometallics* **1997**, *16*, 2798–2807.
- (29) von H. Spence, R. E.; Piers, W. E.; Sun, Y.; Parvez, M.; MacGillivray, L. R.; Zaworotko, M. J. *Organometallics* **1998**, *17*, 2459–2469.
- (30) von H. Spence, R. E.; Parks, D. J.; Piers, W. E.; MacDonald, M.-A.; Zaworotko, M. J.; Rettig, S. J. *Angew. Chem., Int. Ed. Engl.* **1995**, *34*, 1230–1233.
- (31) Chen, C.; Kehr, G.; Frhlich, R.; Erker, G. *J. Am. Chem. Soc.* **2010**, *132*, 13594–13595.
- (32) Douthwaite, R. E. *Polyhedron* **2000**, *19*, 1579–1583.
- (33) Černý, R.; Filinchuk, Y.; Hagemann, H.; Yvon, K. *Angew. Chem., Int. Ed.* **2007**, *46*, 5765–5767.
- (34) Massey, A. G.; Park, A. J. *J. Organomet. Chem.* **1964**, *2*, 245–250.
- (35) Park, D. J.; Piers, W. E.; Yap, G. P. A. *Organometallics* **1998**, *17*, 5492–5503.
- (36) Scott, V. J.; Celenligil-Cetin, R.; Ozerov, O. V. *J. Am. Chem. Soc.* **2005**, *127*, 2852–2853.
- (37) Remenar, J. F.; Lucht, B. L.; Collum, D. B. *J. Am. Chem. Soc.* **1997**, *119*, 5567–5572.